Effect of ^{3}He Impurities on the Nonclassical Response to Oscillation of Solid ^{4}He

E. Kim,[1,*] J. S. Xia,[2,3] J. T. West,[1,†] X. Lin,[1] A. C. Clark,[1] and M. H. W. Chan[1]

[1]*Department of Physics, The Pennsylvania State University, University Park, Pennsylvania 16802, USA*
[2]*Department of Physics, University of Florida, Gainesville, Florida 32611, USA*
[3]*National High Magnetic Field Laboratory (NHMFL), Tallahassee, Florida 32310, USA*

(Received 17 October 2007; published 14 February 2008)

We have investigated the influence of impurities on the possible supersolid transition in ^{4}He by systematically enriching isotopically pure samples with ^{3}He. The addition of ^{3}He broadens the onset of nonclassical rotational inertia and shifts it to higher temperature, suggesting that the phenomenon is correlated with the condensation of ^{3}He atoms onto the dislocation network in solid ^{4}He.

DOI: 10.1103/PhysRevLett.100.065301 PACS numbers: 67.80.−s, 61.72.Hh, 61.72.J−, 61.72.Lk

The prospect of superfluidity in solids raises fundamental questions about our knowledge of condensed matter systems. Thus, the possible existence [1,2] of a supersolid phase in ^{4}He has led to a great deal of excitement in experimental and theoretical communities. In spite of intense activity in recent years the microscopic mechanism for the phenomenon is still not understood.

The observation of nonclassical rotational inertia (NCRI) in solid helium was first reported in a torsional oscillator (TO) experiment with the solid confined within porous Vycor glass [1]. The NCRI was detected as a drop in the resonant period τ_0 of the TO. An intriguing result of this experiment is the extreme sensitivity to ^{3}He impurities. When a minute concentration of ^{3}He ($x_3 \approx 10$ ppm) was present the NCRI fraction (NCRIF) showed a 20% decrease (where NCRIF equals the apparent superfluid mass decoupling divided by the total mass loading of the solid helium sample). The onset temperature T_O increased from ~175 mK to ~300 mK. T_O and NCRIF continued to increase and decrease, respectively, until the signal became undetectable at just $x_3 = 0.1\%$.

NCRI has also been reported in TO measurements on bulk solid ^{4}He [2–5]. All studies except one [5] investigated solid samples grown from commercially available ultrahigh purity (UHP) ^{4}He using the blocked capillary (BC) method. The temperature dependence of NCRIF in UHP ^{4}He (both in the bulk [2–5] and in porous media [1,6]) is qualitatively reproducible. With decreasing temperature, NCRI gradually emerges from the background and then rapidly increases before reaching a constant value below a point of saturation T_S. The values of T_O and T_S typically fluctuate by a factor of 2. In contrast, NCRIF varies widely [4], from 0.03% to at least 20%. It has been suggested that this reflects the degree of disorder in the solid, with higher quality crystals having a smaller NCRIF. However, although superior growth techniques tend to reduce NCRIF in a particular TO, it can still vary by a factor of 10 in large crystals grown at constant pressure in two different cells [5].

A different method to study the effects of disorder is to introduce point defects into the crystal. In view of the sensitivity of the phenomenon to ^{3}He at the parts per million level [1], we have carried out a systematic study in the bulk phase in which the ^{3}He concentration was varied from below 1 ppb up to 30 ppm. Two different torsional oscillators were fabricated for this experiment. Measurements of ^{4}He samples with $1\ \text{ppb} \leq x_3 \leq 129$ ppb were carried out at the high-B and -T facility of NHMFL at the University of Florida employing a TO (TOF) with $\tau_0 = 0.771$ ms and mechanical quality factor $Q = 1 \times 10^6$. The cylindrical sample space in TOF has a height, $h = 0.50$ cm, and a diameter, $d = 1.00$ cm. The period increases by $\Delta\tau_0 = 3940$ ns upon filling the cell with solid helium at 60 bar. Concentrations in the range, $70\ \text{ppb} \leq x_3 \leq 30$ ppm, were studied at Penn State with another TO (TOP) having $\tau_0 = 1.277$ ms, $Q = 5 \times 10^5$, $h = 0.64$ cm, $d = 0.76$ cm, and $\Delta\tau_0 = 1170$ ns.

The isotopically-pure gas came from the U.S. Bureau of Mines. Similarly purified gas was analyzed [7] and found to have $x_3 < 1$ ppb. There is some uncertainty [8] in the exact concentration of the UHP ^{4}He. For calculating mixture concentrations we used $x_3 = 300$ ppb for the commercial UHP gas and $x_3 = 1$ ppb for the isotopically-pure gas. Samples with $x_3 < 300$ ppb were prepared by mixing appropriate amounts of the 1 and 300 ppb gases. Samples with $x_3 > 300$ ppb were prepared by mixing 300 ppb gas with pure ^{3}He. To avoid contamination from residual ^{4}He new capillary and room temperature gas handling systems were constructed. Measurements in each cell started with samples of the lowest x_3, followed by studies of progressively higher concentrations. The pressure of the solid is determined using an *in situ* resistive strain gauge (resolution ≈ 0.5 bar) attached directly to the outer wall of the TO. The BC method was used for all samples resulting in pressures of 60 ± 5 bar. Data were taken during warming scans at low oscillation speeds ($v_0 \leq 10\ \mu\text{m s}^{-1}$).

Figure 1(a) shows NCRIF as a function of temperature for a solid sample with $x_3 = 1$ ppb. NCRI appears below $T_O \approx 80$ mK and saturates below $T_S = 28$ mK. A small dissipation peak is observed with a peak temperature, $T_P = 32$ mK. For $T > T_S$, NCRIF initially drops rapidly and then exhibits a much slower decay to zero between

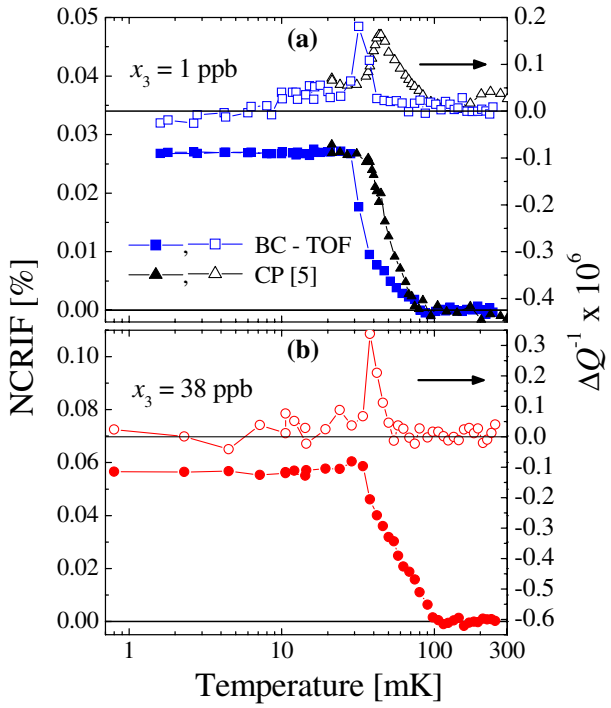

FIG. 1 (color online). (a) Comparison of 1 ppb samples from TOF and Ref. [5]. To qualitatively compare the temperature dependencies, NCRIF and ΔQ^{-1} (dissipation) data for the CP sample [5] are divided by 12 and 5, respectively. No additional T dependence is found below T_S. (b) Ultralow temperature scan of a 38 ppb sample from TOF.

40 mK and 80 mK. Measurements down to 1 mK reveal no additional features below T_S. Similar behavior is seen at $x_3 = 38$ ppb [see Fig. 1(b)]. Data from a sample ($x_3 =$ 1 ppb) grown at constant pressure (CP) in a different cell [5] are also shown in Fig. 1(a). Although the onset temperatures of the two samples are nearly identical, the CP sample (expected to be of much higher quality than the BC sample) shows a sharper transition near T_O.

In Fig. 2 we examine the x_3 dependence of NCRIF (at $T \approx 20$ mK) for both this study and for other data obtained at Penn State. Despite the significant shift from cell to cell, the consistent trend is that NCRIF first increases with the increasing x_3 and then decreases with further ^{3}He enrichment beyond $\sim$1 ppm.

In Fig. 3 we have plotted the normalized NCRIF in solid samples with different x_3 versus a logarithmic temperature scale. Both the NCRIF and ΔQ^{-1} (not shown) curves become increasingly broad and shift to higher temperature with increasing ^{3}He concentration. Over a limited temperature range (less than one third of a decade) we find for some samples a linear dependence of NCRIF on $\log[T]$. However, rounding at high and/or low temperature occurs in most samples, which prevents us from concluding that the decay of NCRIF with temperature is purely exponential. The rounding also makes it difficult to precisely determine T_O and T_S. Therefore, to quantitatively compare

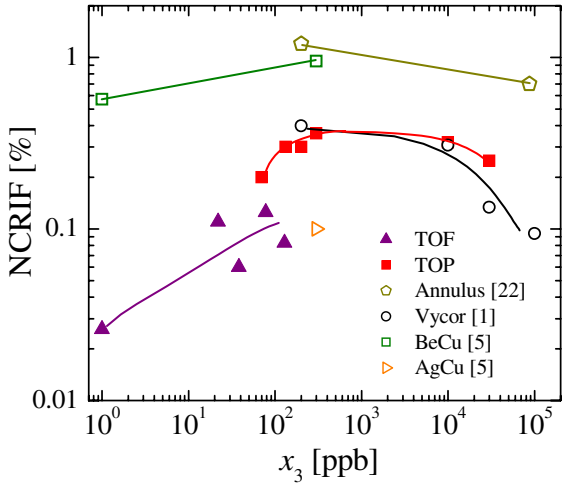

FIG. 2 (color online). x_3 dependence of NCRIF for BC samples obtained in this study and in other TO's from our laboratory. There appears to be an optimal concentration of $\sim$1 ppm, where NCRIF reaches a maximum value.

the temperature dependencies in Fig. 3 we plot the temperatures, T_x [see Figs. 3(d)–3(f)], at which the normalized NCRIF is x% (where $x = 10$, 50, or 90) of the low temperature limiting value. At low x_3 the dissipation peak temperature $T_P \approx T_{50}$. As x_3 increases so does T_P, but less

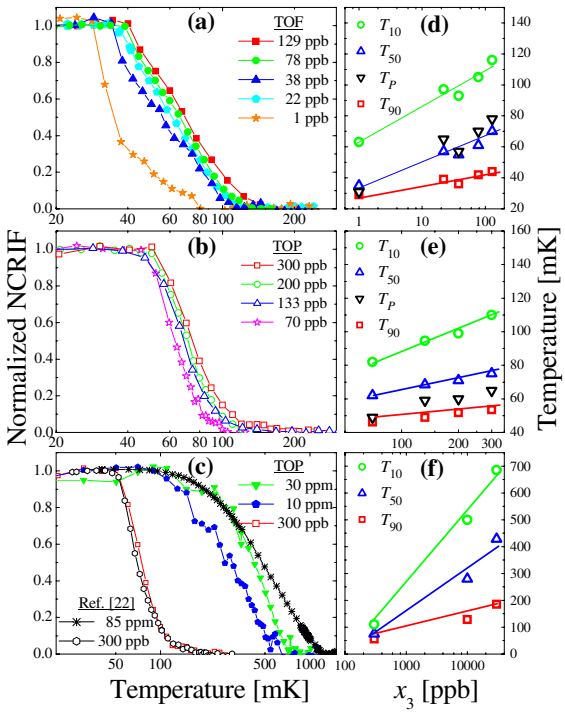

FIG. 3 (color online). T dependence of NCRIF (normalized by the value at $\sim$20 mK) for different x_3 grown in (a) TOF and (b) TOP. (c) T dependence for $x_3 \geq 300$ ppb. Two traces obtained with an annular cell [22] are also shown. (d),(e),(f) The right three panels show the x_3 dependencies of the characteristic temperatures extracted from the adjacent plots.

dramatically than T_{50}. The broadening of the dissipation peak with increasing x_3 is such that no well-defined peak is observable at the highest concentrations. We have compiled the values of T_{50} from this and other experiments into Fig. 4.

A nonsuperfluid mechanism that we have considered to explain the TO experiments is phase separation of the dilute ^{3}He $-$ ^{4}He mixtures. We show in Fig. 4 the phase separation boundary according to both experiments [9,10] and theory [11]. The discrepancy at high x_3 (even for T_{90}) distinguishes the TO results from phase separation. Although the theoretical boundary at low x_3 crosses the datapoints from this study, there is no experimental evidence [10,12] of phase separation for $x_3 < 27$ ppm.

It has been proposed [13] that the dependencies of NCRI on temperature, velocity, and ^{3}He are the result of a vortex liquid phase, with the true supersolid transition occurring at $T \ll T_O$. In this context, the high temperature tail reflects the finite response time of vortices in the sample to oscillatory motion. The broadening with increasing x_3 (see Fig. 3) is due to the slowed vortex motion when ^{3}He atoms attach to the normal cores and get dragged along with the vortices. The accompanying dissipation peak signifies the matching of the TO resonant frequency and the optimal rate at which vortices can respond to changes in the velocity field. Thus, the x_3 dependence of T_P (which is similar to that of T_x) may be a direct probe of the drag force caused by ^{3}He impurity atoms. The complete saturation of NCRIF below T_S indicates that, if there is a supersolid transition in

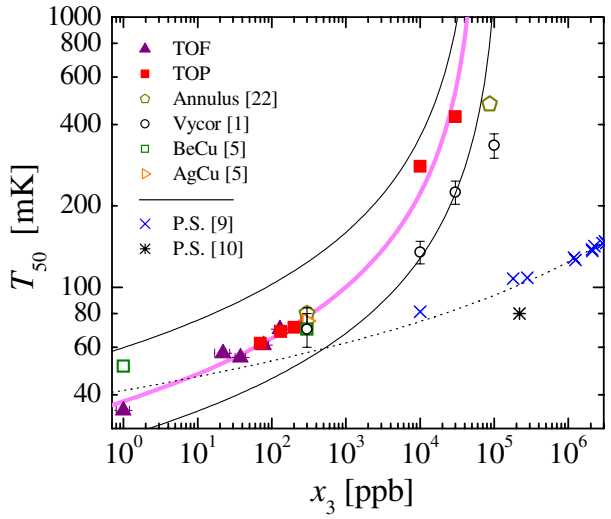

FIG. 4 (color online). T_{50} versus x_3. Relative to T_{50}, values of T_{10} and T_{90} (excluded for clarity) are shifted vertically upward by ~60% and downward by ~25%, respectively. From top to bottom, the three solid lines represent the condition, $T_{IP} = T_x$, for $x = 10$, 50, and 90. To apply Eq. (1) we assume that all samples have the same L_N (and Λ). The fitting parameters are listed in Table I. The theoretical phase separation boundary [11] (dotted line), anchored by pressure [9] and ultrasound [10] measurements, is inconsistent with the TO data.

^{4}He, the critical temperature T_C is either less than 1 mK (i.e., below the temperature range of study) or is marked by the appearance of NCRI such that $T_S < T_C < T_O$.

The connection between a vortex tangle and a superfluid dislocation network has been discussed recently [14]. In one theoretical study [15], in which an analogy is made between entangled dislocations and a vortex glass, ^{3}He impurity atoms play a key role in stabilizing disorder and promoting superfluidity. Thus, another process that may be relevant is the condensation (evaporation) of ^{3}He atoms onto (from) dislocation lines within the sample upon cooling (warming) [16,17]. Dislocations in solid ^{4}He form a random three-dimensional network in which the lines intersect with one another to form a vast number of nodes, which are essentially immobile. In contrast, the line segments between nodes can move readily in stress fields. When an oscillating stress field is imposed, the dislocation segments vibrate with little or no damping below 1 K [18]. The network is characterized by the total line density Λ (total dislocation line length per unit volume) and network loop length L_N between nodes. From ultrasound measurements of single crystals [16,18,19], it is found that $0.1 < \Lambda L_N^2 < 0.3$, where $\Lambda \approx 1 \times 10^6$ cm^{-2} and $L_N \approx 5$ μm. In crystals grown with the BC method it is expected that Λ will increase and L_N will decrease. At low temperature ^{3}He atoms bind to the dislocations with an energy E_B and act as additional pinning centers. There is a crossover from network-pinning to impurity-pinning when the average distance L_{IP} between condensed ^{3}He atoms becomes less than L_N. The x_3-dependent temperature at which this occurs can be obtained from the average pinning length [16], and is of the form

$$T_{IP} = -2E_B\left(\ln\left[\frac{x_3^2 L_{IP}^3 E_B}{4\mu b^6}\right]\right)^{-1}. \quad (1)$$

Here, b is the magnitude of the Burger's vector of a dislocation and μ is the shear modulus of ^{4}He.

In order to reveal the possible connection between impurity-pinning and the observed x_3 dependence of NCRI, we identify the crossover point with each characteristic temperature (i.e., $T_{IP} = T_x$) and fit the measured T_{10}, T_{50}, and T_{90} by adjusting L_{IP} and E_B. Figure 4 demonstrates the accuracy of Eq. (1) in describing the data. The best fit parameters (see Table I) are consistent with the literature [16,17]. If we fix $E_B = 0.42$ K for all three data sets, the curves calculated from Eq. (1) deviate from the observed T_{10} and T_{90} for $x_3 < 100$ ppb. However, such a protocol results in L_{IP} that are longest for T_{10} and shortest for T_{90}, as expected [16]. The same qualitative trends are observed in the Vycor data. However, the above analysis is inappropriate due to the solid ^{4}He morphology [20] and overall complexity of the system. If we naively apply Eq. (1) we get parameters similar to those in Table I (eg., for T_{50} we get $L_{IP} = 0.5$ μm, which is much greater than the 7 nm pore size).

TABLE I. Parameters for Eq. (1) associated with the three curves in Fig. 4. Uncertainties in E_B are 10%, and in L_N they are 20%. There is also a possible systematic error in defining [8] $x_3 = 300$ ppb for UHP ^{4}He. However, if we instead use $x_3 =$ 200 or 500 ppb, the new parameters fall within the error margins above. Dislocation densities were calculated by setting $L_N \approx L_{\mathrm{IP}}$ and $\Lambda L_N^2 = 0.2$. The resulting values are greater than those typical of single crystals, as expected.

T_x [K]	E_B [K]	L_{IP} [μm]	Λ [10^6 cm^{-2}]
T_{10}	0.66	1.7	7
T_{50}	0.42	1.9	6
T_{90}	0.33	1.3	12

The fact that the characteristic temperatures of NCRI can be described by Eq. (1) indicates that the observed x_3 dependence is correlated with the impurity-pinning of dislocations. The temperature independence for 1 mK $< T <$ T_S (see Fig. 1) suggests that below the saturation point the dislocations are completely pinned. It is surprising that even just 1 ppb (or less [7]) of impurities can immobilize the dislocations. As a sample of a fixed x_3 is warmed above T_S the continual evaporation of ^{3}He atoms from the dislocation network softens the solid, which may concomitantly destroy NCRI. A dramatic increase at low temperature of the shear modulus in solid ^{4}He has in fact been observed recently [21]. The anomaly exhibits the same qualitative (and perhaps semiquantitative) dependencies on temperature, ^{3}He concentration (for $x_3 = 1, 85$, and 300 ppb), and stress amplitude ($\propto v_0$ in the TO experiments) as NCRI.

In conclusion, we found that the x_3 dependence of the characteristic temperatures of NCRI are consistent with the binding of ^{3}He atoms to dislocations. The absence of any temperature dependence below $\sim$28 mK in isotopically-pure samples suggests that the most likely phase transition point lays between T_S and T_O.

We thank P. W. Anderson and J. R. Beamish for their advice, and J. R. Beamish and J. A. Lipa for providing us with isotopically pure ^{4}He. E. K. and M. H. W. C. also acknowledge the illuminating discussions at workshops held at the Kavli Institute of Theoretical Physics at UCSB, the Aspen Center for Physics, Keio University, and the Outing Lodge sponsored by the Pacific Institute of Theoretical Physics. The work at PSU was supported by NSF Grants No. DMR-0207071 and No. DMR-0706339. The State of Florida and NSF No. DMR-9527035 funded research carried out at UF.

*Permanent address: Physics Department, Korea Advanced Institute of Science and Technology, 373-1 Guseong-dong, Yuseong-gu, Daejeon 305-701, Korea.
†jtw11@psu.edu

[1] E. Kim and M. H. W. Chan, Nature (London) **427**, 225 (2004).
[2] E. Kim and M. H. W. Chan, Science **305**, 1941 (2004).
[3] E. Kim and M. H. W. Chan, Phys. Rev. Lett. **97**, 115302 (2006); A. S. C. Rittner and J. D. Reppy, Phys. Rev. Lett. **97**, 165301 (2006); Y. Aoki, J. C. Graves, and H. Kojima, Phys. Rev. Lett. **99**, 015301 (2007); A. Penzev, Y. Yasuta, and M. Kubota, J. Low Temp. Phys. **148**, 677 (2007); M. Kondo, S. Takada, Y. Shimbayama, and K. Shirahama, J. Low Temp. Phys. **148**, 695 (2007).
[4] A. S. C. Rittner and J. D. Reppy, Phys. Rev. Lett. **98**, 175302 (2007).
[5] A. C. Clark, J. T. West, and M. H. W. Chan, Phys. Rev. Lett. **99**, 135302 (2007).
[6] E. Kim and M. H. W. Chan, J. Low Temp. Phys. **138**, 859 (2005).
[7] See BM-RI-8054 (1975) and BM-RI-9010 (1986). Further information on these technical reports can be found at www.osti.gov/energycitations/.
[8] The concentration varies by the source, but is on the order of 10^{-7} for gas taken from oil wells. For example, see C. J. Ballentine, R. K. O'Nions, and M. L. Coleman, Geochim. Cosmochim. Acta **60**, 831 (1996) or Ref. [30] in R. H. Brown, Origins **25**, 55 (1998). From these articles the range is 200 ppb $< x_3 <$ 500 ppb.
[9] A. N. Gan'shin *et al.*, Low Temp. Phys. **26**, 869 (2000).
[10] J. M. Goodkind, AIP Conf. Proc. **850**, 329 (2006).
[11] D. O. Edwards and S. Balibar, Phys. Rev. B **39**, 4083 (1989).
[12] X. Lin, A. C. Clark, and M. H. W. Chan, Nature (London) **449**, 1025 (2007).
[13] P. W. Anderson, Nature Phys. **3**, 160 (2007).
[14] M. Boninsegni, A. B. Kuklov, L. Pollet, N. V. Prokof'ev, B. V. Svistunov, and M. Troyer, Phys. Rev. Lett. **99**, 035301 (2007).
[15] E. Manousakis, Europhys. Lett. **78**, 36002 (2007).
[16] I. Iwasa and H. Suzuki, J. Phys. Soc. Jpn. **49**, 1722 (1980).
[17] M. A. Paalanen, D. J. Bishop, and H. W. Dail, Phys. Rev. Lett. **46**, 664 (1981).
[18] R. Wanner, I. Iwasa, and S. Wales, Solid State Commun. **18**, 853 (1976).
[19] I. Iwasa, K. Araki, and H. Suzuki, J. Phys. Soc. Jpn. **46**, 1119 (1979).
[20] D. Wallacher, M. Rheinstaedter, T. Hansen, and K. Knorr, J. Low Temp. Phys. **138**, 1013 (2005).
[21] J. Day and J. R. Beamish, Nature (London) **450**, 853 (2007).
[22] E. Kim, Ph.D. thesis, The Pennsylvania State University, 2004.